

# Diosgenin Selective Molecularly Imprinted Polymers with Acrylonitrile-methacrylic Acid Matrix

STEFAN-OVIDIU DIMA<sup>1,2\*</sup>, ANDREI SARBU<sup>2\*</sup>, TANASE DOBRE<sup>1</sup>, VIOLETA PURCAR<sup>2</sup>, CRISTIAN-ANDI NICOLAE<sup>2</sup>

<sup>1</sup> Politehnica University of Bucharest, Faculty of Applied Chemistry and Material Science, Mass Transfer Department, 1-7 Gheorghe Polizu Str., 011061, Bucharest, Romania

<sup>2</sup> National Research and Development Institute for Chemistry and Petrochemistry ICECHIM, Polymers Department, 202 Splaiul Independentei, 060021, Bucharest, Romania

A new set of molecularly imprinted polymers (MIPs), based on acrylonitrile: methacrylic acid (AN:MAA) matrix, selective for diosgenin, was synthesized and characterized. The target molecule, diosgenin, is an important anticancer and antileukemia bioactive compound. The phase inversion method, an emerging and insufficiently studied preparation method, was used to prepare 0.5 mm spherical MIPs. Three copolymers of acrylonitrile with methacrylic acid were synthesized by radical copolymerization: AN:MAA 90:10, 80:20 and 70:30 and used for diosgenin imprinting. The imprinted materials were analysed by elemental analysis (EA), attenuated total reflectance infrared spectroscopy (ATR FT-IR), RAMAN spectroscopy, size exclusion chromatography (SEC), thermogravimetric analysis (TGA), differential scanning calorimetry (DSC) and batch rebinding tests. The affinity for the template, expressed as the imprinting factor *IF*, decreases in the order MIP-AN:MAA-80:20 > MIP-AN:MAA-90:10 > MIP-AN:MAA-70:30, meaning that -COOH functional groups have an important role in the imprinting process. Too much methacrylic groups, however, do not exhibit the highest affinity, maybe due to the steric obstruction of methyl groups and to a less stability of the structure by decreasing the AN ratio.

**Keywords:** molecular imprinting, diosgenin, phase inversion, acrylic copolymers, MIPs

Molecularly imprinted polymers (MIPs) are a type of synthesized materials with specific recognition ability for one special type of molecule (sometimes group of molecules) called template [1-5]. The template is either chosen because of its special properties for humankind, or it is imposed by safety regulations to be separate or removed from products intended for human or animal consumption. In comparison with the common absorbents such as active carbon, the MIPs have higher reusability, selectivity and lower consumption [6,7].

Molecular recognition is crucial for the functioning of

living systems, where biological macromolecules including proteins (enzymes, antibodies and receptors), nucleic acids and saccharides play decisive roles in biological activities [8-10].

In the effort to obtain host molecules with precise recognition of guest species, the design, synthesis and evaluation of supramolecules are being intensively investigated in laboratories throughout the world. The MIPs synthesis implies either non-covalent interactions or reversible covalent interactions between the molecular template and the functional monomers, as represented in figure 1 [11].

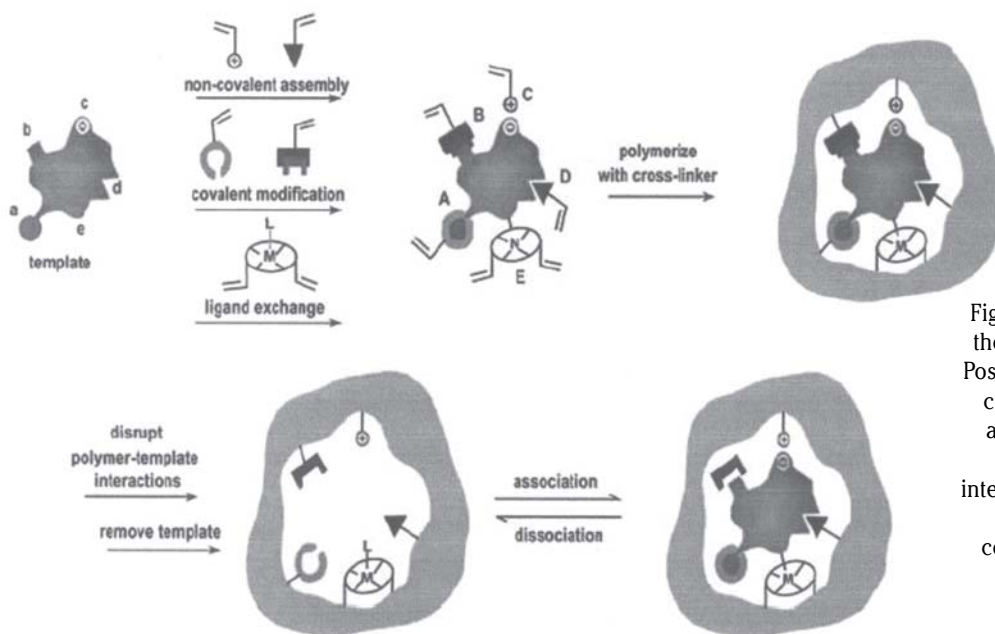


Fig. 1. Schematic representation of the molecular imprinting process. Possible interactions: (A) reversible covalent bond(s), (B) covalently attached polymerizable binding groups, (C) electrostatic interactions, (D) hydrophobic or van der Waals interactions, or (E) coordination with a metal center

\* email: andr.sarbu@gmail.com; phd.ovidiu.dima@gmail.com

After the imprinting step, the template is removed by chemical reaction or extraction technique. Then binding sites which are complementary in size, geometry and functional groups orientation to the template molecule are exposed. Because of their outstanding advantages in comparison with biological receptors, including high specific recognition, stability in organic solvents, ease and low cost for preparation, MIPs have been widely used in liquid chromatography [12], chemical and biological sensors [13,14], chiral resolution [15], antibody simulation [16], drug delivery and screening [17-19].

Various methods to separate bioactive compounds from complex phytoextracts are tested in many recent papers [20-22], MIPs based methods being among the most selective ones. Diosgenin, a steroid sapogenin with estrogenic bioactivity [23] found in complex phytoextracts, presents interest because can reduce the cholesterol from blood (serum cholesterol) and can also treat leukaemia, colon cancer and climacteric syndrome [24,25].

The interaction of a molecularly imprinted polymer with its template can be described by a model of reversible binding, characterized by dissociation equilibrium constant. The key parameters can be deduced from concentration-dependent binding isotherms, and quantified most accurately by computer-assisted, non-linear regression analysis or fitted by the linear subtraction method [26].

The earliest method of linearization of ligand-binding data according to Scatchard is still frequently employed. Scatchard analysis is an effortless and straightforward way to recognize multiple classes of binding sites and provides the most compact graphical presentation of binding data [27]. The hypothesis that all binding sites are alike does not apply in most developed MIPs and usually Scatchard plots fit to a curve which degree of curvature contains information about the affinity distribution of binding sites [28].

The aim of this paper is to present the obtaining and characterization of diosgenin imprinted acrylonitrile-methacrylic acid (AN:MAA) pearls. Diosgenin was imprinted in three AN:MAA copolymer matrices (90:10, 80:20 and 70:30 %) by phase inversion and the characterization of the obtained MIPs was done using world-wide recognized techniques: elemental analysis (EA), attenuated total reflectance infrared spectroscopy (ATR FT-IR), RAMAN spectroscopy, size exclusion chromatography (SEC), thermogravimetric analysis (TGA), differential scanning calorimetry (DSC) and Scatchard analyses from batch rebinding tests.

## Experimental part

The sample given names represent a code that suggestively describes all its main characteristics. The copolymers are coded as AN:MAA plus the ratio between monomers (example: AN:MAA-90:10). The imprinted pearls have the prefix MIP (example: MIP-AN:MAA-90:10), the non-imprinted pearls have the prefix NIP (example: NIP-AN:MAA-90:10), while the extracted pearls have the prefix MIP and the suffix Ex (example: MIP-AN:MAA-90:10Ex).

### Synthesis of copolymer matrix

Three acrylonitrile (AN) - methacrylic acid (MAA) copolymers were synthesized by radical copolymerization in aqueous environment, initiated with the redox system: potassium persulfate – sodium

metabisulfite.

The synthesis recipe was (mass percent):  
-monomers (AN+MAA) concentration: 15%,  
-potassium persulfate (PK) concentration (relative to monomers): 0.5%,  
-sodium metabisulfite (MS) concentration (relative to monomers): 0.5%,  
-H<sub>2</sub>SO<sub>4</sub> concentration (relative to monomers): 0.3%,  
-polymerization temperature: 45°C,  
-polymerization time: 90 min under continuous stirring.

The initiators (MS and PK) were dissolved separately in water.

The weight ratios between monomers were 90:10, 80:20 and 70:30. The order of adding the chemicals in the reactor was: water, AN, MAA, MS aqueous solution. Nitrogen was sparged into solution for 10 – 15 min to remove oxygen, which is polymerization inhibitor for AN. Then PK aqueous solution with H<sub>2</sub>SO<sub>4</sub> was added. The reaction mixture was kept at constant temperature using a thermostated bath, under mixing, 90 min.

### Pre-imprinting step

The copolymers were dissolved in dimethylformamide (DMF), having 8, 10 and 12% concentration (copolymer in DMF) and 5% template concentration (related to the polymer).

First, the template (diosgenin) was dissolved 15 min in DMF at 70°C and, after that, the copolymer was added and let the steric arrangements to form during 45 min, under stirring.

### Imprinting step = phase inversion step

The moment when the copolymer structure stabilises around template molecules represents the imprinting step. Depending on the type of medium, the phase inversion can be wet or dry, but in this case the wet phase inversion was chosen because the solvent (DMF) has a high boiling point.

For diosgenin imprinted polymers, seven phase inversion bath compositions were tried, namely: dimethylformamide: water (50:50, 40:60, 30:70), isopropyl alcohol: water (50:50, 40:60, 30:70) and distillate water. The result was that the fastest phase inversion occurred in water.

The pearl shape was obtained by a dripping technique. The solution was aspirate in a syringe and then it was trickled in the coagulation bath. The pearls were maintained 30 min in the coagulation bath (to stabilize the structure).

### Template extraction

The template was extracted by washing method, using a microdose pump working with 6 mL/min hot solvent (ethanol, 60°C), during 30 min. The washing method was efficient because the template is completely removed, as the HPLC analysis showed.

### Analytic techniques

In order to characterize the structure and morphology of diosgenin MIPs, different complementary methods were used. Elemental analysis (EA) was realized using a Perkin Elmer 2400 Series II CHNS/O Analyzer with thermal conductivity detector (TCD). Triplicate determinations of elements in AN:MAA 90:10, 80:20 and 70:30 copolymers were performed, in all their forms: copolymer, MIP (imprinted), NIP (non-imprinted) and MIP-Ex (extracted). The combustion temperature was 975°C. Attenuated total reflectance infrared spectro-

scopy (ATR FT-IR) was done using the instrument TENSOR 37, which has the spectral range between 7500 and 370  $\text{cm}^{-1}$ , a high sensitivity DLATGS detector with KBr window and a resolution better than 0.6  $\text{cm}^{-1}$ . RAMAN analyses were performed on a DXR Thermo Scientific Raman microscope at 780 nm, aperture 25  $\mu\text{m}$ , 14 mW laser power, 2 scans for sample. Size exclusion chromatography (SEC HPLC) was used to analyse the presence of the template inside the polymer pearls. It was performed using an Agilent Technologies 1200 series, equipped with a PLgel 5  $\mu\text{m}$  MIXED-C column, dimensions L x Di = 300 x 7.5 mm, and refractive index detector (RID). The method used dimethylformamide as solvent at 1 mL/min flow and 25°C. The volume of an injected sample was 20  $\mu\text{L}$ . Thermogravimetric analyses (TGA) were performed using a TA Q5000 IR Instrument, under nitrogen, up to 700°C, with a linear heating rate of 10°C/min. Differential scanning calorimetry (DSC) analyses were done on a TA Q2000 DSC Instrument. The method consisted in three steps: first heating from 20 to 170°C with a heating rate of 10°C/min, cooling to 20°C with the same rate, 10°C/min, and then second heating up to 170°C with the same heating rate.

#### Batch rebinding tests

The binding capacity of the imprinted polymers with varying concentrations of analyte (5 concentrations: 0.1, 0.2, 0.3, 0.4 and 0.5% diosgenin in ethanol) was evaluated from batch binding studies. 20 vials, 5 for each type of polymer pearls (MIP-AN:MAA-90:10, MIP-AN:MAA-80:20, MIP-AN:MAA-70:30, NIP-AN:MAA-90:10, NIP-AN:MAA-80:20 and NIP-AN:MAA-70:30), each one containing 100 mg pearls were contacted with 8 mL from the initially prepared ethanol solutions (0.1-0.5% diosgenin). In order to analyse the free template, supernatant samples were taken at 0.1, 0.2, 0.3, 0.4, 0.5, 1.5, 3, 6, 12 and 24 h. The concentration of free diosgenin was determined using a calibration curve that correlates the peak area (A) obtained by SEC with the concentration of diosgenin, assessed experimentally

and presented as equation 1.

$$c(\%) = 9.5 \cdot 10^{-7} \cdot A - 1.1 \cdot 10^{-3} \quad (1)$$

#### Results and discussions

From elemental analysis were obtained data of the percentage of elements contained by the copolymer samples presented in table 1. The AN:MAA copolymers were analyzed in all preparation steps: before imprinting (AN:MAA), after imprinting (MIP-AN:MAA) and after template extraction (MIP-AN:MAA Ex). Also, a comparison between different batches for the same copolymer was done (b1-batch 1, b2-batch 2).

Elemental analysis confirmed the theoretical calculation of AN:MAA copolymers, the initial ratio of monomers and also the imprinting (the presence of template) and the extraction of the template (by changes in elements amount).

The FT-IR spectroscopy offers much information regarding the bounds formed in the imprinting step and also proves the extraction of template from the pores.

The notations in the legend of figure 2 correspond to non-imprinted pearls (NIP-signal 1), diosgenin (the template-signal 2), molecularly imprinted AN:MAA 90:10 pearls (MIP-signal 3) and extracted MIPs (MIP-Ex - signal 4).

Using an on-line updated data base for spectroscopy, it was identified the first important peak at 2860  $\text{cm}^{-1}$ , corresponding to associated -O-H stretching vibration (table 2), characteristic to the template (diosgenin). At this wavelength an important shoulder is present in MIP (signal 3 in fig. 2), that almost disappear in MIP-Ex, and is very small in NIP. At this wavelength can also be recorded intramolecular H-bond (possible H-bonds between the template and the copolymer matrix).

The next observation is at the wavelength corresponding to -Ca $\equiv$ N stretching vibration, 2244  $\text{cm}^{-1}$ . In NIP and MIP-Ex the absorbance is higher than in MIP, signifying that the acrylonitrile nitrile groups are more free to move and vibrate than they are in MIP, were -Ca $\equiv$ N can make hydrogen bonds with template -OH groups (according to the imprinting mechanism). Also

No.	Sample	Carbon, %		Hydrogen, %		Nitrogen, %		Oxygen, %	
		Theo.	Exp.	Theo.	Exp.	Theo.	Exp.	Theo.	Exp.
1	AN:MAA 90:10b1	66.07	65.01	5.86	6.43	24.87	23.59	3.20	4.97
2	AN:MAA 90:10b2	66.07	64.33	5.86	6.35	24.87	24.33	3.20	4.99
3	AN:MAA 80:20b1	64.43	64.51	6.04	6.69	23.49	21.68	6.04	7.12
4	AN:MAA 80:20b2	64.43	64.31	6.04	6.65	23.49	21.53	6.04	7.51
5	AN:MAA 70:30b1	62.96	62.13	6.20	6.80	22.26	19.29	8.59	11.78
6	AN:MAA 70:30b2	62.96	62.21	6.20	6.73	22.26	19.32	8.59	11.74
7	MIP-AN:MAA-90:10	65.79	65.74	6.65	6.56	18.17	19.02	9.39	8.68
8	MIP-AN:MAA-90:10Ex	66.07	66.03	5.86	5.91	24.87	24.58	3.20	3.48
9	MIP-AN:MAA-80:20	64.87	64.55	8.39	8.19	17.43	18.04	9.31	9.22
10	MIP-AN:MAA-80:20Ex	64.43	64.44	6.04	6.72	23.49	22.91	6.04	5.93
11	MIP-AN:MAA-70:30	63.67	63.45	8.10	8.24	16.74	17.15	11.48	11.16
12	MIP-AN:MAA-70:30Ex	62.96	62.86	6.20	6.22	22.26	21.91	8.59	8.98

**Table 1**  
ELEMENTAL ANALYSIS OF  
THE PREPARED  
COPOLYMERS:  
THEORETICAL AND  
EXPERIMENTAL VALUES.

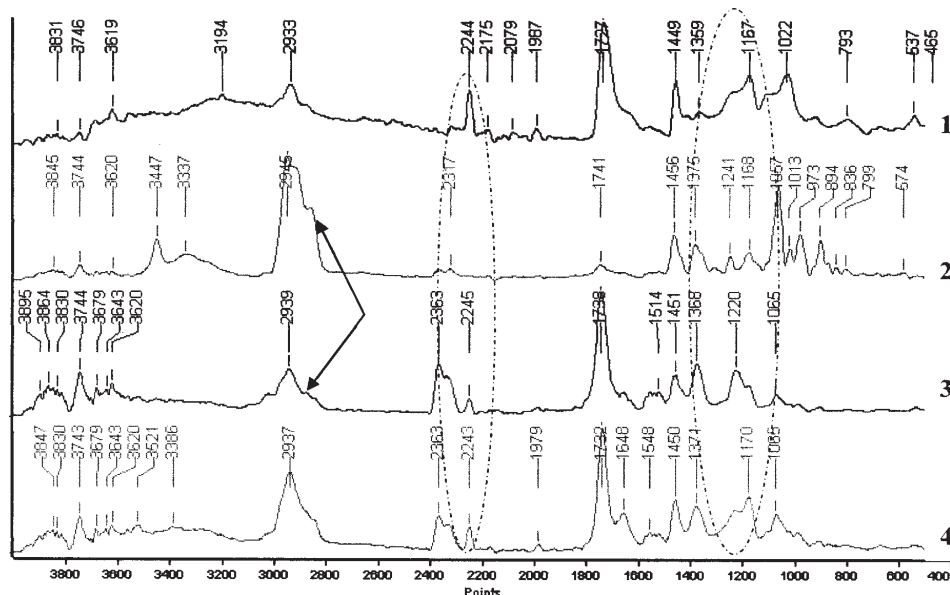


Fig. 2. FTIR spectra of: 1) NIP-AN:MAA-80:20; 2) Diosgenin; 3) MIP-AN:MAA-80:20; 4) MIP-AN:MAA-80:20Ex.

NIP	Diosgenin	MIP	MIP-Ex	Assignment
2933	2945	2939	2937	C-H stretching vibration- asym
-	<b>2860</b>	<b>2860</b>	-	<b>associated -O-H stretching vibration</b>
<b>2244</b>	-	<b>2244</b>	<b>2243</b>	<b>-C≡N stretching vibration</b>
<b>1727</b>	<b>1741</b>	<b>1738</b>	<b>1732</b>	<b>C=O stretching vibration in COOH</b>
1449	1456	1451	1450	C-H deformation vibration
<b>1211</b>	<b>1211</b>	<b>1220</b>	<b>1220</b>	<b>C-O stretching n vibration in alcohols</b>
<b>1167</b>	<b>1168</b>	<b>1065</b>	<b>1170</b>	<b>C-O stretching n vibration in alcohols</b>

Table 2  
IMPORTANT WAVELENGTHS IN  
AN:MAA - DIOSGENIN  
SELECTIVE MIPs

a displacement in  $-C\equiv N$  peak position (from  $2245\text{ cm}^{-1}$  to  $2243\text{ cm}^{-1}$ ) after the template extraction suggests possible disappearance of some template-copolymer matrix bonds.

A very active region in shifting is the C=O and C-O areas of vibration ( $1727\text{ cm}^{-1}$ ,  $1211\text{ cm}^{-1}$ ,  $1167\text{ cm}^{-1}$ ). This is an important argument that the COOH functional groups, present in copolymer matrix, interact with the OH functional groups of diosgenin. In the region  $1170\text{--}1220\text{ cm}^{-1}$  the peak aspect changes after template extraction, the MIP-Ex absorbance being similar with the NIP absorbance, but with a little shift (from  $1167\text{ cm}^{-1}$  in NIP to  $1170\text{ cm}^{-1}$  in MIP-Ex). In this way, the extraction of template is put in evidence.

Figure 3 presents the Raman spectra for the three copolymers used in the molecular imprinting process (AN:MAA 90:10, 80:20 and 70:30). The variation of methacrylic ratio used for the polymer matrix is visible in the region  $2920\text{--}2950\text{ cm}^{-1}$  (the C-H stretching vibration - asymmetric) and in the region  $1455\text{--}1313\text{ cm}^{-1}$ , the CO region.

The imprinting can be demonstrated also from Raman spectra of MIP pearls before extraction (MIP-AN:MAA-80:20) containing 5% diosgenin, and after extraction (MIP-AN:MAA-80:20Ex), as it can be seen in figure 4.

Diosgenin makes hydrogen and van der Waals bonds with the matrix functional groups and influences the area  $1200\text{--}2000\text{ cm}^{-1}$ . After diosgenin extraction with ethanol, the MIP Ex has similar spectrum as NIP (non-imprinted).

The thermogravimetric analyses were presented in

two forms: as weight loss variation (fig. 5) and as derivative weight variation with the temperature (fig. 6). The thermal degradation compares the three AN:MAA copolymers and the corresponding homopolymers: polyacrylonitrile (PAN) and polymethacrylic acid (PMAA).

The homopolymer PAN is the most thermally stable, this being acrylonitrile main role in the copolymer matrix, to create a rigid structure, while the methacrylic acid has the role of binding the template using the carboxyl

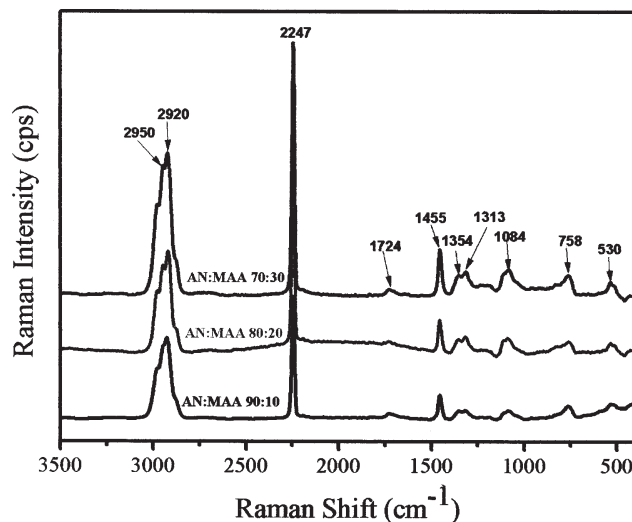


Fig. 3. Raman spectra for the three AN:MAA copolymers

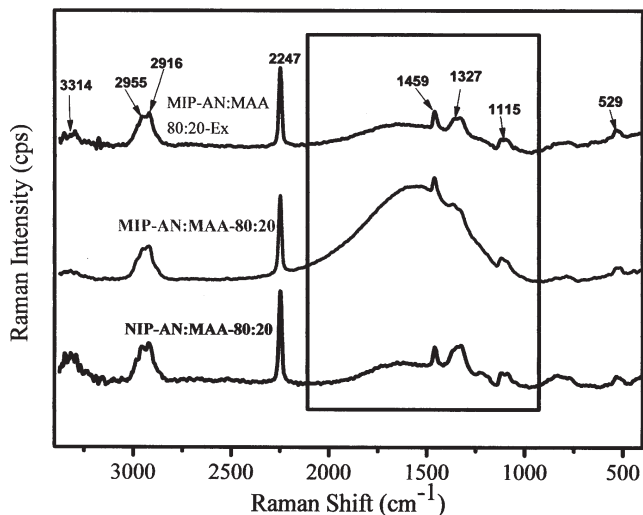


Fig. 4. Comparison between Raman spectra of imprinted pearls (MIP-AN:MAA-80:20), extracted pearls (MIP-AN:MAA-80:20Ex) and non-imprinted pearls (NIP-AN:MAA-80:20).

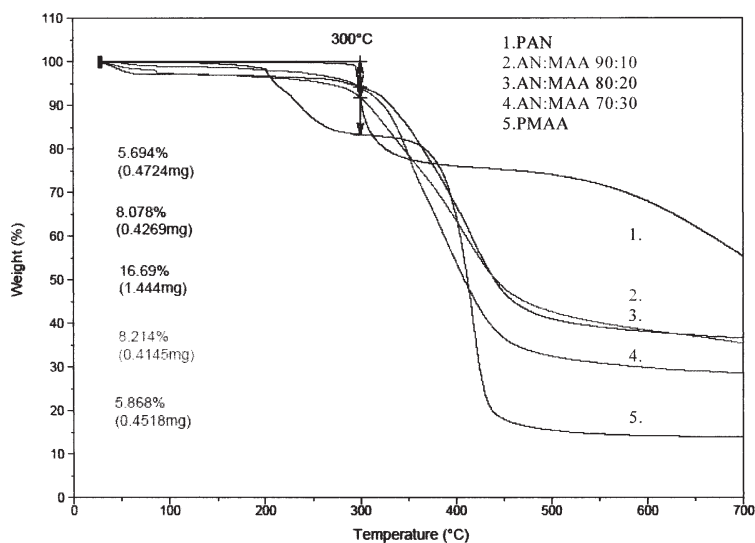


Fig. 5. TGA analysis showing the weight loss of AN:MAA copolymers and the corresponding homopolymers PAN and PMAA

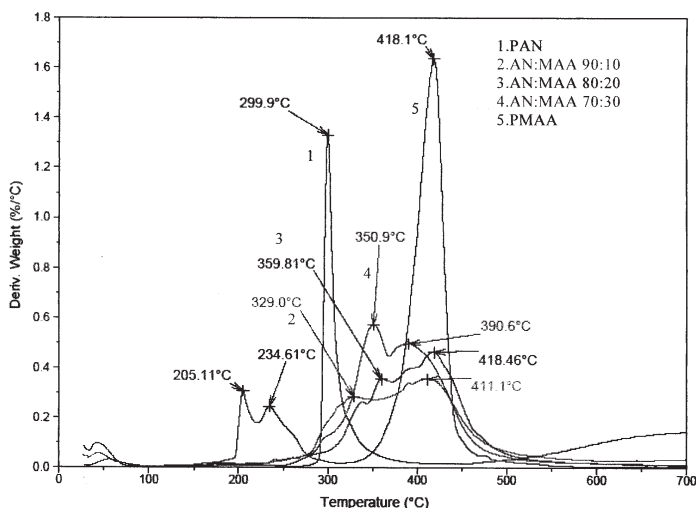


Fig. 6. DTG analysis showing the derivative weight loss of AN:MAA copolymers and for the corresponding homopolymers PAN and PMAA.

functional group. All polymers loose in the initial step water or solvents, up to 100°C. The homopolymer PMAA is the less stable, having the highest weight loss. And this weakness is found in the copolymer with the highest ration of methacrylic acid.

The derivative weight diagram presented in figure 6 shows that the thermal degradations take place in two main steps for all copolymer materials. For the PMAA the first main thermal event starts around 200°C, has the maximum speed of degradation at 205°C and stops around 300°C. The AN:MAA copolymers start the thermal degradation around 270°C. In this temperature range, the acrylic acid decomposes by dehydration of the acid

groups forming anhydride, which decompose later by decarboxylation [29]. On the decomposing of acrylic acid is overlaid the effect of acrylonitrile thermal transformations, which between 270 - 350°C suffers processes of dehydrogenation and stabilization by cyclization. The last step of degradation, 350-500°C is characteristic to acrylonitrile aromatization [30,31].

From the thermal analysis, a conclusion can be draw regarding the influence of the ratio between monomers. Experimental thermograms indicate that the methacrylic acid has catalytic effect on copolymers' thermal degradation because a higher amount of MAA leads to a faster degradation.

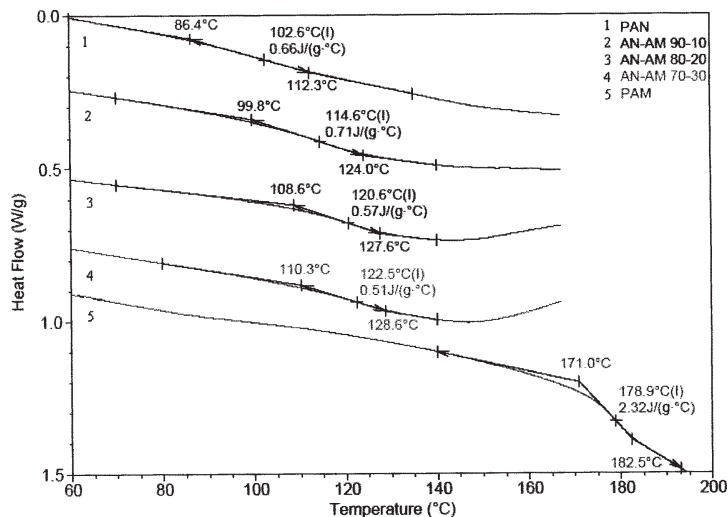


Fig. 7. DSC analysis for AN:MAA copolymers and corresponding homopolymers.

The differential scanning calorimetry (DSC) is useful to find the transition temperatures ( $T_g$  – glass transition temperature) for the prepared materials. The AN:MAA copolymers have the  $T_g$  between the homopolymers'  $T_g$  (fig. 7), 104°C (for PAN) and 179°C (for PMAA), this being an evidence that the prepared copolymers are statistic, not block. And the alternation of nitrile and carboxyl functional groups, as found in statistic copolymers, is a condition for good affinity sites in MIPs.

From the batch rebinding experiments, a very useful diagram, called Scatchard diagram, is obtained. For this diagram the amount of template bound on copolymer pores,  $B$ , is determined by subtraction of the free template,  $F$ , from the total amount,  $T$ . And if the ratio  $B/F$  is represented against  $B$  (equation 2), the Scatchard diagram is obtained (fig. 8).

$$\frac{B}{F} = K \cdot B_{\max} - K \cdot B \quad (2)$$

The Scatchard diagram for MIPs appears as a curve for which two tangents can be traced (fig. 9). The significance of the two traces with different slopes is that each one represents a type of binding site inside the imprinted polymer [32]. For MIP-AN:MAA-80:20 the first trace has a bigger slope, which signify that the adsorption in those pearls is faster. In the diagram only one NIP was plotted (NIP-AN:MAA-70:30) because the other one has similar aspect. In NIP only one type of binding sites, with no affinity for the template, are determined. NIP pearls also have adsorption capacity because of the preparation method, which implied the use of the same porogen (DMF). The calculated parameters are given in table 3.

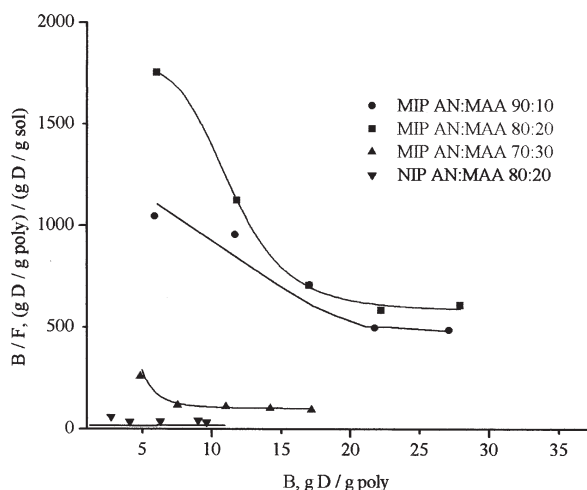


Fig. 8. Scatchard diagram for MIP AN:AA 90:10, MIP AN:AA 80:20 and NIP AN:AA 90:10

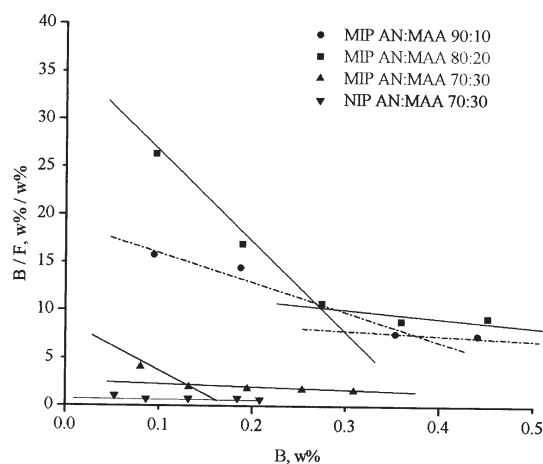


Fig. 9. Finding the parameters in Scatchard diagram for MIP-AN:MAA-90:10, MIP-AN:MAA-80:20, MIP-AN:MAA-70:30 and NIP-AN:MAA-70:30

Polymer	$K_1$	$B_{\max 1}$	$K_2$	$B_{\max 2}$
MIP-AN:MAA-90:10	30.9	0.617	5.7	1.675
NIP-AN:MAA-90:10	3.5	0.321	-	-
MIP-AN:MAA-80:20	95.1	0.381	10.1	1.315
NIP-AN:MAA-80:20	3.4	0.348	-	-
MIP-AN:MAA-70:30	49.3	0.175	3.0	0.855
NIP-AN:MAA-70:30	1.7	0.484	-	-

**Table 3**  
COMPARING THE SCATCHARD  
PARAMETERS FOR THE AN:MAA MIPs  
AND NIPs

**Table 4**  
IMPRINTING FACTORS AND YIELD OF IMPRINTING FOR AN:MAA MIPs

T, %, initial concentration	MIP-AN:MAA-90:10		MIP-AN:MAA-80:20		MIP-AN:MAA-70:30	
	IF	YI	IF	YI	IF	YI
<b>0.1</b>	2.5	92.90	3.1	95.63	1.76	76.44
<b>0.2</b>	2.4	92.28	3.3	93.36	1.85	59.61
<b>0.3</b>	2.1	89.86	3.0	89.85	1.75	58.11
<b>0.4</b>	2.0	86.15	2.9	87.95	1.58	56.28
<b>0.5</b>	1.9	88.98	2.9	88.41	1.79	54.46
<i>Mean value</i>	<i>2.2</i>	<i>89.41</i>	<i>3.1</i>	<i>91.04</i>	<i>1.75</i>	<i>60.98</i>

Two representative parameters for the imprinting process will be forward calculated: the imprinting factor (IF) with equation (3) and the yield of imprinting (YI) with equation (4).

$$IF = \frac{qB_{MIP}}{qB_{NIP}} \quad (3)$$

$$YI = \frac{B}{B+F} \cdot 100 \quad (4)$$

were  $qB_{MIP}$  is the quantity of template adsorbed (bound) by MIP, g template;

$qB_{NIP}$  is the quantity of template adsorbed (bound) by NIP, g template;

B, %, the template bound from the initial solution;

F, %, the free template found in solution.

The results obtained are shown in table 4.

### Conclusions

Three molecularly imprinted polymers, based on AN:MAA matrix and diosgenin as template, were prepared by phase inversion method. The copolymerization proceeded in good conditions, the elemental analysis proving that the experimental elemental composition is closed to the theoretical one.

The ATR-FTIR spectroscopy evidenced characteristic peaks proving the presence of the template in the copolymer matrix and proving the complete extraction of template. Very important observation is that in the imprinting process, the both types of functional groups -Ca≡N and -COOH available in copolymer matrix are involved.

The template, diosgenin, was attached to the matrix using its free -OH functional groups. The bounds are non-covalent: hydrogen bounds and van der Waals, and are reversible. They break in the extraction conditions, ethanol at high temperature (60°C), and rebind in adsorption conditions (room temperature, batch contacting).

The affinity for the template, expressed as the imprinting factor IF, decrease in the order MIP-AN:MAA-80:20 > MIP-AN:MAA-90:10 > MIP-AN:MAA-70:30, meaning that both -COOH and -CN functional groups have an important role in the imprinting process. Too much methacrylic groups, however, do not exhibit the

highest affinity, maybe due to the steric obstruction of methyl groups and to a less stability of the structure by decreasing the AN ratio.

### References

1. AZODI-DEILAMI, M.A.S., ASADI, E., SHARIATINIA, Z., J. Mater. Sci.: Mater. Med., DOI 10.1007/s10856-012-4623-5, 2012.
2. ZHANG, C., HUANG, K., YU, P., LIU, H., Sep. Purif. Technol., 87, 2012, p. 127.
3. NICOLESCU, T.V., SARBU, A., GHIUREA, M., DONESCU, D., U.P.B. Sci. Bull. B, 73 (1), 2011, p. 163.
4. DIMA, S.O., DOBRE, T., SARBU, A., GHIUREA, M., BRADU, C., U.P.B. Sci. Bull. B, 2009, 71 (4), p. 21.
5. MEOUCHE, W., BRANGER, C., BEURROIES, I., DENOYEL, R., MARGAILLAN, A., Macromol. Rapid. Comm., DOI: 10.1002/marc.201200039, 2012.
6. CIRILLO, G., CURCIO, M., PARISI, O.I., PUOCI, F., IEMMA, F., SPIZZIRRI, U.G., RESTUCCIA, D., PICCI, N., Food. Chem., 125, 2011, p. 1058.
7. NICOLESCU, T. V., SARBU, A., DIMA, S.O., NICOLAE, C., DONESCU, D., J. Appl. Polym. Sci., DOI 10.1002/app.37528, 2012.
8. PAULING, L. J., J. Am. Chem. Soc., 62, 1940, p. 2643.
9. SANDU, T., SARBU, A., CONSTANTIN, F., OCNARU, E., VULPE, S., DUMITRU, A., IOVU, H., Rev. Roum. Chim., 56 (9), 2011, p. 875.
10. KRYSZCIO, D.R., PEPPAS, N.A., Acta. Biomater., 8, 2012, p. 461.
11. PUOCI, F., IEMMA, F., PICCI, N., Curr. Drug Delivery, 5, 2008, p. 85.
12. FERRER, I., LANZA, F., TOLOKAN, A., HORVATH, V., SELLERGRIN, B., HORVAI, G., BARCELO, D., Anal. Chem., 72, 2000, p. 3934.
13. AVILA, M., ZOUGAGH, M., RIOS, A., ESCARPA, A., Trends Anal. Chem., 27, 2008, p. 54.
14. GONZALEZ, G.P., HERNANDO, P.F., ALEGRIA, J.S.D., Anal. Chim. Acta, 638, 2009, p. 209.
15. QUAGLIA, M., DE, L.E., SULITZKY, C., MASSOLINI, G., SELLERGRIN, B., Analyst, 126, 2001, p. 1495.
16. KARMALKAR, R.N., KULKARNI, M.G., MASHELKAR, R.A., J. Control. Release, 43, 1997, p. 235.
17. DUARTE, A.R.C., CASIMIRO, T., AGUIAR-RICARDO, A., SIMPLICIO, A.L., DUARTE, C.M.M., J. Supercrit. Fluids, 39, 2006, p. 102.
18. YE, L., MOSBACH, K., J. Am. Ceram. Soc., 123, 2001, p. 2901.
19. HUGON-CHAPUIS, F., MULLOT, J.U., TUFFAL, G., HENNION, M.C., PICHON, V., J. Chromatogr. A, 1196-1197, 2008, p. 73.
20. YUAN, Y., WANG, Y., HUANG, M., XU, R., ZENG, H., NIE, C., KONG, J., Analyst. Chim. Acta, 695 (1-2), 2011, p. 63.
21. KISS, B., POPA, D.S., HANGANU, D., POP, A., LOGHIN, F., Rev. Roum. Chim., 55 (8), 2010, p. 459.

22. DIMA, S.O., SARBU, A., DOBRE, T., BRADU, C., ANTOHE, N., RADU, A.L., NICOLESCU, T.V., LUNGU, A., *Mat. Plast.*, **46**, no. 4, 2009, p. 224.
23. ZHAI, C., LU, Q., CHEN, X., PENG, Y., CHEN, L., DU, S., *J. Chromat. A*, 1216, 2009, p. 2254.
24. LEPAGE, C., LEGER, D.Y., BERTRAND, J., MARTIN, F., BENEYTOU, J.L., LIAGRE, B., *Cancer. Lett.*, 301, 2011, p. 193.
25. KOMESAROFF, P.A., BLACK, C.V., CABLE, V., SUDHIR, K., *Climacteric.*, 4, 2001, p. 144.
26. GOMEZ-PINEDA, L.E., PINA-LUIS, G.E., CUAN, A., GARCIA-CALZON, J.A., DIAZ-GARCIA, M.E., *React. Funct. Polym.*, 71, 2011, p. 402.
27. GARCIA-CALZON, J.A., DIAZ-GARCIA, M.E., *Sens. Actuat. B*, 123, 2007, p. 1180.
28. CORTON, E., GARCIA-CALZON, J.A., DIAZ-GARCIA, M.E., *J. Non-Cryst. Solids*, 353, 2007, p. 974.
29. SILEO, E.E., MORANDO, P.J., BAUMGARTNE, E.C., BLESIA, M.A., *Thermochim Acta*, 184 (2), 1991, p. 295.
30. WU, G.P., LU, C.X., LING, L.C., LU, Y.G., *Polym. Bull.*, 62, 2009, p. 667.
31. RADU, A.L., SARBU, A., MOTOC, S., MARA, L., FRUTH-OPRISAN, V., GAREA, S.A., DIMA, S.O., NECHIFOR, G., SARBU, L., IOVU, H., *Mat. Plast.*, **47**, no. 2, 2010, p. 167.
32. ATHIKOMRATTANAKUL, U., KATTERLE, M., GAJOVIC-EICHELMANN, N., SCHELLER, F.W., *Talanta*, 84, 2011, p. 274

---

Manuscript received: 12.12.2011